Coupled transport and reaction kinetics control the nitrate source-sink function of hyporheic zones

Jay P. Zarnetske,[1] Roy Haggerty,[2] Steven M. Wondzell,[3] Vrushali A. Bokil,[4] and Ricardo González-Pinzón[5]

Received 20 January 2012; revised 24 September 2012; accepted 26 September 2012; published 7 November 2012.

[1] The fate of biologically available nitrogen (N) and carbon (C) in stream ecosystems is controlled by the coupling of physical transport and biogeochemical reaction kinetics. However, determining the relative role of physical and biogeochemical controls at different temporal and spatial scales is difficult. The hyporheic zone (HZ), where groundwater–stream water mix, can be an important location controlling N and C transformations because it creates strong gradients in both the physical and biogeochemical conditions that control redox biogeochemistry. We evaluated the coupling of physical transport and biogeochemical redox reactions by linking an advection, dispersion, and residence time model with a multiple Monod kinetics model simulating the concentrations of oxygen (O_2), ammonium (NH_4), nitrate (NO_3), and dissolved organic carbon (DOC). We used global Monte Carlo sensitivity analyses with a nondimensional form of the model to examine coupled nitrification-denitrification dynamics across many scales of transport and reaction conditions. Results demonstrated that the residence time of water in the HZ and the uptake rate of O_2 from either respiration and/or nitrification determined whether the HZ was a source or a sink of NO_3 to the stream. We further show that whether the HZ is a net NO_3 source or net NO_3 sink is determined by the ratio of the characteristic transport time to the characteristic reaction time of O_2 (i.e., the Damköhler number, Da_{O2}), where HZs with $Da_{O2} < 1$ will be net nitrification environments and HZs with $Da_{O2} \gg 1$ will be net denitrification environments.* Our coupling of the hydrologic and biogeochemical limitations of N transformations across different temporal and spatial scales within the HZ allows us to explain the widely contrasting results of previous investigations of HZ N dynamics which variously identify the HZ as either a net source or sink of NO_3. Our model results suggest that only estimates of residence times and O_2 uptake rates are necessary to predict this nitrification-denitrification threshold and, ultimately, whether a HZ will be either a net source or sink of NO_3.

Citation: Zarnetske, J. P., R. Haggerty, S. M. Wondzell, V. A. Bokil, and R. González-Pinzón (2012), Coupled transport and reaction kinetics control the nitrate source-sink function of hyporheic zones, *Water Resour. Res.*, *48*, W11508, doi:10.1029/2012WR011894.

1. Introduction

1.1. Background

[2] Bioavailable forms of nitrogen (N), such as nitrate (NO_3), are necessary for aquatic ecosystem productivity, and the availability of this reactive N often limits ecosystem productivity [*Jones and Holmes*, 1996]. However, human alterations to the global N budgets have more than doubled the supply of reactive N over the last century which in turn has caused increasingly negative impacts on water quality and aquatic ecosystems (e.g., biodiversity loss [*Sala et al.*, 2000], water quality degradation [*Smith*, 2003], accelerated global carbon and N cycling rates [*Gruber and Galloway*, 2008], and increased hypoxic events [*Diaz and Rosenberg*, 2008]). Streams are particularly important locations in the landscape for the reactive N cycle, because they integrate many N sources and control N export to downgradient systems via internal N source and sink processes (e.g., mineralization of organic forms of N and denitrification of NO_3,

[1]School of Forestry & Environmental Studies, Yale University, New Haven, Connecticut, USA.
[2]College of Earth, Ocean and Atmospheric Sciences and Institute for Water and Watersheds, Oregon State University, Corvallis, Oregon, USA.
[3]Corvallis Forestry Sciences Laboratory, Pacific Northwest Research Station, Corvallis, Oregon, USA.
[4]Department of Mathematics, Oregon State University, Corvallis, Oregon, USA.
[5]College of Earth, Ocean and Atmospheric Sciences and Water Resources Graduate Program, Oregon State University, Corvallis, Oregon, USA.

Corresponding author: J. P. Zarnetske, School of Forestry & Environmental Studies, Yale University, 195 Prospect St., New Haven, CT 06511, USA. (jay.zarnetske@yale.edu)

©2012. American Geophysical Union. All Rights Reserved.
0043-1397/12/2012WR011894

*This sentence is correct here. The article as originally published appears online.

respectively). Consequently, there is a need to determine the key factors controlling sources and sinks of reactive N in stream ecosystems. Unfortunately, N transformations in aquatic ecosystems are typically complex and couple multiple N species in both space and time. Thus, it is difficult to predict if a particular component of an aquatic system will function as a net source or sink, and over what critical temporal and spatial scales it will function. In this study, we focus on how and why stream–groundwater (hyporheic, HZ) interactions are important for coupled N transformations in stream systems, and how they function as both a source and a sink of NO_3 to downgradient aquatic systems.

[3] HZs are locations in the streambed and adjacent surficial aquifers where stream and groundwater mix. HZs are known to be important locations for N transformations in streams [e.g., *Duff and Triska*, 1990; *Holmes et al.*, 1994] because they contain strong hydrologic and biogeochemical gradients [*Jones and Holmes*, 1996; *Baker et al.*, 2000a]. These gradients lead to different redox conditions, which in turn control the conditions under which many biogeochemical reactions can occur [*Hedin et al.*, 1998]. In particular, redox conditions control where and when nitrification and denitrification can occur. Both nitrification and respiratory denitrification are facilitated by microbes. Nitrification represents the chemoautotrophic oxidation of NH_4 to NO_3 and thus is a source of NO_3 to aquatic ecosystems. Denitrification, on the other hand, is the reduction of dissolved NO_3 to dinitrogen gas (N_2), which can subsequently return to the atmosphere (Table 1). Denitrification is a particularly important N transformation in streams, because it represents the one true sink of NO_3 in aquatic ecosystems. Therefore, there is much interest in identifying when and where denitrification will be the dominant fate of NO_3 versus when and where NO_3 production via nitrification will dominate in a system.

[4] There are both physical and biogeochemical conditions of HZs that regulate N biogeochemistry. The physical factors regulate the supply rate of solutes and include advection, dispersion, hydraulic conductivity, and flow path length. These physical conditions determine the solute flux through the HZ and the characteristic residence time distributions of the water and solutes in the HZ. The biogeochemical factors are oxygen (O_2), labile dissolved organic carbon (DOC), dissolved organic nitrogen (DON), inorganic nitrogen (NH_4 and NO_3), temperature, and pH. Most nitrifying microbes require O_2 and NH_4, while denitrifiers require anoxic conditions, a DOC source to serve as an electron donor, and a supply of NO_3 to serve as an electron acceptor [*Hedin et al.*, 1998; *Baker et al.*, 2000b]. In many systems, nitrification and denitrification are tightly coupled because nitrification consumes O_2 while producing NO_3, and both anoxic conditions and NO_3 availability will stimulate denitrification [e.g., *Duff and Triska*, 1990, *Holmes et al.*, 1996; *Sheibley et al.*, 2003] as long as there are sources of labile DOC available [e.g., *Sobczak et al.*, 2003; *Zarnetske et al.*, 2011b]. Natural heterogeneity in streams leads to unique combinations of both the physical and biogeochemical conditions which in turn result in unique N source and sink conditions. This heterogeneity makes it hard to identify a priori the function of an HZ, so it is important to identify and account for the key components of the HZ N cycle.

[5] The meta-analysis by *Seitzinger et al.* [2006] and recent experimental and modeling studies [e.g., *Zarnetske et al.*, 2011a; *Marzadri et al.*, 2011; *Bardini et al.*, 2012] showed that net nitrification and denitrification are coupled and related to residence time in the HZ, where net nitrification dominates short residence times and net denitrification dominates long residence times. There are also a growing number of numerical modeling studies of groundwater–surface water exchange that have focused on how the physical sediment and hydrodynamic conditions can regulate NO_3 flux and transformations across two-dimensional (2-D) HZ features (e.g., bed forms and meander bars). For example, *Cardenas et al.* [2008] and *Boano et al.* [2010] showed that varying these physical transport conditions can change the biogeochemical zonation of where specific redox conditions occur in the subsurface, including NO_3 reduction. Expanding on these modeling studies, *Marzadri et al.* [2011] and *Bardini* et al., [2012] showed that varying only the physical transport can shift a streambed from net nitrification to net denitrification system and that the hydrologic variability may be more important than reaction substrate (DOC and NO_3) variability.

[6] Theoretically, linking NO_3 dynamics to residence time helps simplify some of the above-stated complexities in the biogeochemical substrate limitations while offering an explanation as to why previous field studies of HZ NO_3 dynamics showed inconsistent HZ functioning—as either a source of NO_3 via nitrification or a sink of NO_3 via denitrification. For example, *Holmes et al.* [1994] showed that short residence time oxic HZ flow paths within a desert N-limited stream function as net nitrification systems, while much longer residence time anoxic HZ flow paths of a more temperate N-rich river function as a net denitrification system [*Pinay et al.*, 2009]. Larger-scale synoptic sampling of spatially diverse stream ecosystems also shows heterogeneity in whether the stream sediment functions as a net source or sink of NO_3 given catchment setting and land use type [*Inwood et al.*, 2005; *Arango and Tank*, 2008]. Accounting for the differences in residence time should collapse some of the variability seen between these systems with respect to HZ N source-sink processes [*Seitzinger et al.*, 2006, *Zarnetske et al.*, 2011a; *Marzadri et al.*, 2011, *Bardini et al.*, 2012].

Table 1. Stoichiometry of Microbially Mediated Processes in the Reactive Transport Model[a]

Reaction Processes	General Stoichiometric Reaction Equation	Free Energy ΔG^{0b} (kJ mol^{-1})
Aerobic Respiration	$CH_2O + O_2 \rightarrow CO_2 + H_2O$	−501
Nitrification	$O_2 + (1/2)NH_4^+ \rightarrow (1/2)NO_3^- + H^+ + (1/2)H_2O$	−181
Denitrification	$CH_2O + (4/5)\,NO_3^- + (4/5)\,H^+ \rightarrow (7/5)\,H_2O + (2/5)\,N_2 + CO_2$	−476
Microbial NH_4^+ Uptake[c]	$5CH_2O + HCO_3^- + NH_4^+ \rightarrow C_5H_7NO_2 + 4H_2O + CO_2$	

[a]Adapted from *McCarty* [1971], *Stumm and Morgan* [1981], and *Hedin et al.* [1998].
[b]Assumes 25°C and pH = 7.
[c]Cell synthesis (as $C_5H_7NO_2$) with NH_4^+ as the N source.

1.2. Objectives and Conceptual Framework of Study

[7] Our goal is to construct a general but practical theoretical framework to predict the NO_3 source and sink potentials of a given stream HZ. To do this we need to identify the fundamental subset of physical and biogeochemical factors controlling N transformations in HZs (see section 1.1 for factors). The theoretical studies discussed above clearly illustrate that variability in the hydrologic kinetics play an important role in determining the HZ function as a source or sink of NO_3. Field and laboratory studies show that N reaction kinetics are controlled by the availability of terminal electron donors (labile DOC) and acceptors (O_2 and NO_3) and environmental factors such as temperature and pH. Representing all of these hydrologic and reaction kinetics in numerical models is possible; however, it is less feasible and practical to do so when scaling HZ function across a river system or making comparisons between several different HZs. Clearly there is a need to develop a minimally parameterized, scalable model to make robust predictions about the net source or sink function of HZs in streams.

[8] We hypothesize that the net source or sink function of a HZ will be primarily a function of the characteristic residence time scales of water and solute in the HZ and the characteristic reaction (uptake) rate time scales of O_2. In other words, the potential function of an HZ as a source or sink of NO_3 will be primarily controlled by the supply and demand rates of O_2, because O_2 controls the redox conditions which regulate where and when nitrification and denitrification occur [*Seitzinger*, 1988; *Hedin et al.*, 1998]. Dissolved oxygen is critical to this hypothesis because it is known that O_2 availability in saturated sediment strongly inhibits denitrification [e.g., *Terry and Nelson*, 1975; *van Kessel*, 1977; *Christensen et al.*, 1990], but when O_2 becomes scarce, NO_3 is thermodynamically favorable as the terminal electron acceptor (Table 1 [*Champ et al.*, 1979; *Hedin et al.*, 1998]). Furthermore, we focus on the O_2 uptake (respiration) rate because it is regulated by the labile DOC availability in the system, where low labile DOC availability will limit O_2 respiration rates [*Pusch and Schwoerbel*, 1994; *Baker et al.*, 2000b]. Oxygen uptake rate is also a function of temperature and pH conditions [*Stumm and Morgan*, 1981; *Hedin et al.*, 1998]. Therefore, O_2 uptake rates subsume some of the complex dynamics of labile DOC and other physiochemical conditions in a system. Additionally, the logistics of directly measuring or modeling water residence times and oxygen dynamics in HZ systems is easier than that of NO_3 and DOC (e.g., field and experimental tracer tests, groundwater flow models, and O_2 measurement instruments). Consequently, we hypothesize that the Damköhler number for O_2, Da_{O2} (the ratio of O_2 reaction rate time scales to water residence time scales) in an HZ system will be a good indicator of the potential for the HZ to function as a net nitrification or denitrification location in the landscape. We define the Damköhler number for O_2 as

$$Da_{O_2} = \tau * V_{O_2}, \tag{1}$$

where V_{O_2} is the oxygen reaction rate (T^{-1}), τ is the water residence time (T), and $\tau = L/v$, L is the length of the flow path (L), and v is the mean advected water velocity (LT^{-1}).

[9] The Damköhler number is a useful concept for hydrochemical processes that are a function of both transport and reaction rates, because it is a dimensionless number that compares the role of reaction and transport processes within and across systems [*Boucher and Alves*, 1959; *Domenico and Scwhartz*, 1998; *Ocampo et al.*, 2006; *Gu et al.*, 2007; *Boano et al.*, 2010]. In particular, *Ocampo et al.* [2006] and *Gu et al.* [2007] showed that this approach is useful in relating dynamic denitrification rates to transport rates in groundwater environments. Similarly, the recent use of a Lagrangian framework for modeling reactive transport and redox conditions in river meander HZs showed that predictions of NO_3 reduction rates (as well as SO_4, CO_2, and CH_4 reduction) can be made by relating HZ transport time scales to reduction rate time scales [*Boano et al.*, 2010]. However, no previous study has attempted to use this scaling approach to identify the net NO_3 source and sink function, via net nitrification and denitrification, of HZs across variable transport and reaction conditions. Therefore, we expand on our Da_{O_2} hypothesis to explore different conceptual HZ conditions, including more complex biogeochemical reaction kinetics, and the resulting HZ functioning as a net nitrification or denitrification system. First we define the HZ function as a net source or sink by calculating the fraction change in NO_3 mass F_N, between the initial NO_3 concentrations at the beginning N_{in}, and end of the HZ flow path N_{out}:

$$F_N = \frac{N_{out}}{N_{in}}. \tag{2}$$

Thus, F_N ($0 < F_N < \infty$), where a net denitrifying system is ($0 < F_N < 1$) and a net nitrifying system is ($F_N > 1$). Next we can relate the F_N to the Da_{O_2} of a system or flow path (Figure 1), such that we see the characteristic Da_{O_2} of

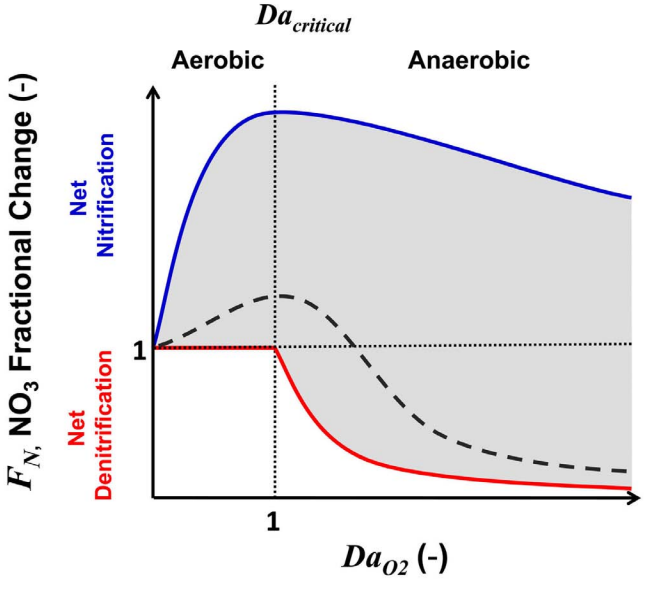

Figure 1. A conceptual model showing how net nitrification and net denitrification potential (F_N) is a function of the Damköhler number Da_{O2} (ratio of characteristic hydrologic transport time scale to biological O_2 uptake time scale). The gray area represents the hypothesized F_N domain for all combinations of hyporheic conditions controlling nitrification and denitrification. The dashed line within the domain represents the conditions observed along hyporheic flow paths of an upland agricultural stream by *Zarnetske et al.* [2011a].

an HZ will control the aerobic and anaerobic domains in the system, and therefore the domains over which net nitrification and denitrification occur. For example, net denitrification will be inhibited at values of $Da_{O_2} < 1$, because this region of a system is where the physical supply rate time scale of O_2 (i.e., $\tau = L/v$) is smaller than the demand rate time scale of O_2 (i.e., V_{O_2}), and therefore will be oxic. This $Da_{O_2} < 1$ domain will promote nitrification if NH_4 is present in addition to inhibiting denitrification. A value of $Da_{O_2} = 1$ represents a critical point in the system when the physical supply time scale is equal to the biological demand time scale, and therefore represents the point in a system where O_2 is exhausted and anaerobic conditions will begin to influence the biogeochemical processes. Lastly, all values of $Da_{O_2} > 1$ represent points in a system where demand exceeds the supply of O_2, and therefore will be anaerobic and have the potential to experience net denitrification if NO_3 and labile DOC are present.

1.3. Approach of Study

[10] We used a numerical one-dimensional, multispecies, reactive N transport model to test the hypothesis and conceptual model (section 1.2 and Figure 1). The model was used to evaluate the coupling of physical transport conditions (advection, dispersion, and residence time) and biogeochemical redox conditions with modified Monod kinetics for O_2, NH_4, NO_3, and DOC. We used a dimensionless form of the model to simulate O_2, NH_4, NO_3, and DOC concentrations profiles for different hyporheic physical and biogeochemical conditions. Using this model we are able to evaluate the broad biogeochemical parameter space associated with substrate limitations on hyporheic N transformations not included in previous studies, while including the key physical transport parameters of advection and dispersion that govern solute transport in an HZs [*Cardenas et al.*, 2008; *Boano et al.*, 2010; *Zarnetske et al.*, 2011a; *Marzadri et al.*, 2011; *Bardini et al.*, 2011].

[11] We used this model to conduct an extensive global Monte Carlo sensitivity analysis of possible model parameter combinations seen in the literature to evaluate the general NO_3 source-sink hypothesis and conceptual model shown in Figure 1. These Monte Carlo simulations explore a broad range of literature values and isolate the fundamental parameters governing the likelihood of simulating a net source or sink system as defined by the resulting values of F_N.

2. Methods

2.1. Model Overview With Transport and Reaction Kinetics

[12] The transport of reactive solutes along hyporheic flow paths was modeled with a one-dimensional advection-dispersion model with multiple Monod biological reactions. This general modeling approach, using both physical transport and reaction kinetics, has been used to model reactive NO_3 reduction and transport in HZ environments [*Sheibley et al.*, 2003; *Gu et al.*, 2007; *Zarnetske*, 2011]. The basic form of the mathematical model is

$$\frac{\partial C_i}{\partial t} = D\frac{\partial^2 C_i}{\partial x^2} - v\frac{\partial C_i}{\partial x} + R_i, \tag{3}$$

where C_i is the concentration of the ith solute (ML^{-3}), D is the dispersion coefficient (L^2T^{-1}), v is the mean advected water velocity (LT^{-1}), and R_i is the biological reaction rate term ($ML^{-3}T^{-1}$) representing the uptake kinetics of the ith solute due to all biogeochemical processes. Dispersion is assumed to be in the form $D = \alpha_L v$, where α_L is the dispersivity.

[13] The modeled biological reactions are aerobic respiration, nitrification, and denitrification (Table 1), and are represented with multiple Monod kinetics in the transport model. The processes of dissimilatory nitrate reduction to ammonium (DNRA) and anaerobic ammonium oxidation (ANAMMOX) can also affect the cycling of nitrate and ammonium in stream sediments [*Burgin and Hamilton*, 2007], but were not modeled. DNRA was not included because its influence on hyporheic inorganic N dynamics is negligible compared to nitrification and denitrification [*Kelso et al.*, 1999; *Puckett et al.*, 2008]. ANNOMOX was not included because the role of ANNOMOX in producing N_2 via the chemoautotrophic oxidation of ammonium and nitrites is probably negligible compared to the role of respiratory denitrification in most freshwater systems [*Burgin and Hamilton*, 2007].

[14] Monod kinetics represents a chain of enzymatically mediated reactions with a limiting step described by Michaelis-Menten kinetics. The reactions in this case can be limited by multiple factors—substrates, electron acceptors, and nutrient availability. Multiple Monod kinetics are preferred over other kinetic models (e.g., instantaneous or zero- and first-order kinetics), because the Monod model does not assume that a biological reaction is instantaneous and it can capture multiple-order (zero-, first-, and mixed-order) behavior of biological reactions [*Bekins et al.*, 1998]. The multiple Monod model was also selected because it is not known a priori when and where a particular reaction is rate limited by substrate or nutrient availability. Following the formulations presented by *Molz et al.* [1986] and *Gu et al.* [2007], the multiple Monod kinetics are modified to be governed by the concentration of substances linked with a reaction—the terminal electron donors and acceptors associated with aerobic respiration, nitrification, and denitrification. The general mathematical form of the Monod model used in this study is

$$R_i = V_k X_j I\left(\frac{C_{ED}}{K_{ED} + C_{ED}}\right)\left(\frac{C_{EA}}{K_{EA} + C_{EA}}\right), \tag{4}$$

where R_i is the total biological reaction for the ith solute (O_2, NH_4, NO_3, or DOC) due to the sum of different reaction components acting on a common ith solute ($ML^{-3}T^{-1}$), V_k is the maximum microbial process reaction rate (T^{-1}) for the kth solute reaction contributing to R_i, where k runs over O_2, NH_4, NO_3, or DOC and can be different from the ith solute, X_j is the biomass of the jth functional microbial group (ML^{-3}) facilitating the different reaction components of aerobic respiration (AR), nitrification (NIT), biological uptake (UP), or denitrification (DN), I is a noncompetitive inhibition factor (–) used to represent inhibition of denitrification given O_2 availability, C_{ED} and C_{EA} are the concentrations of the solutes involved in the reaction (ML^{-3}), K_{ED} and K_{EA} are the half-saturation constants (ML^{-3}), and the subscripts ED and EA designate the

electron donor substrate and the electron acceptor, respectively. For example, using equation (4) the aerobic respiration component of the O_2 reaction $R^*_{O_2}$ is

$$R^*_{O_2} = -V_{O_2} X_{AR} \left(\frac{DOC}{K_{DOC} + DOC}\right)\left(\frac{O_2}{K_{O_2} + O_2}\right), \quad (5)$$

where DOC and O_2 are concentrations of dissolved organic carbon and dissolved oxygen (ML^{-3}), V_{O_2} is the O_2 reaction rate (T^{-1}), K_{DOC} and K_{O_2} are the half-saturation constants for DOC and O_2, respectively (ML^{-3}), and X_{AR} is the biomass of the aerobic respiration functional group (ML^{-3}).

[15] There are two N transforming reactions in the model that are limited by the availability of O_2 nitrification and denitrification. Nitrification requires O_2 and denitrification is noncompetitively inhibited by O_2. The noncompetitive inhibition of denitrification arises from the fact that O_2 is thermodynamically advantageous over NO_3 as an electron acceptor [*Stumm and Morgan*, 1981; *Hedin et al.*, 1998]. Therefore, a noncompetitive uptake inhibition model is included in the transport model. *Segel* [1975] provides a general mathematical form for modeling uptake inhibition for denitrification I (–) for a noncompetitive situation such as the inhibition of denitrification by O_2. The general form is

$$I = \frac{K_I}{K_I + O_2}, \quad (6)$$

where K_I is the inhibition constant for the denitrification reaction (ML^{-3}). Upon inspection of equation (5), it is seen that when $O_2 \ll K_I$ there is negligible inhibition ($I \approx 1$) and when $O_2 \gg K_I$ inhibition is important ($I \approx 0$). Therefore, the denitrification component of the NO_3 reaction $R^*_{NO_3}$ is

$$R^*_{NO_3} = -V_{NO_3} X_{DN} I \left(\frac{DOC}{K_{DOC} + DOC}\right)\left(\frac{NO_3}{K_{NO_3} + NO_3}\right), \quad (7)$$

where NO_3 is the concentration of dissolved nitrate (ML^{-3}), V_{NO_3} is the denitrification rate (T^{-1}), K_{NO_3} is the half-saturation constant for NO_3 (ML^{-3}), and X_{DN} is the biomass of the denitrifiers (ML^{-3}).

[16] We account for the cumulative effects of multiple microbial functional groups acting on a single solute with a specific effective uptake rate for the processes acting on O_2 and NH_4, where V_{O_2} characterizes the effects of O_2 uptake during aerobic respiration and nitrification and V_{NH_4} characterizes the effects of NH_4 uptake by nitrification and microbial assimilation. We assume that bioenergenic relationships based on thermodynamics can be used to partition the V_{O_2} and V_{NH_4} uptake between O_2 demand (R_{O_2}) via aerobic respiration and nitrification reaction components, and NH_4 demand (R_{NH_4}) via nitrification and biological uptake for cell synthesis reaction components (Table 1). Bioenergenics is a useful approach to reducing the complexity of modeling microbial stoichiometry associated oxidation, reduction, and microbial assimilation via cell synthesis processes represented in this study [*McCarthy*, 1971; *Heijnen and Van Dijken*, 1992; *Xiao and Van Briesen*, 2005; *Hedin et al.*, 1998; *Heijnen*, 2010]. The partition coefficient for O_2 demand processes y_{O_2} (–) was calculated based on the known free energy yield ΔG^0 (kJ mol^{-1}), between the two competing processes of aerobic respiration ΔG^0_{AR}, and nitrification ΔG^0_{NIT} in Table 1, such that

$$y_{O_2} = \frac{\Delta G^0_{AR}}{\Delta G^0_{AR} + \Delta G^0_{NIT}}. \quad (8)$$

Therefore, the remaining solute available for the secondary, less energetically preferential, uptake reaction is $1 - y_{O_2}$, assuming the aerobic respiration and nitrification are the dominant removal pathways for O_2. The NH_4 partition coefficient y_{NH_4}, on the other hand, is based upon the bioenergenics and bacterial growth efficiencies, because cell synthesis requires the use of free energy produced via respiration pathways. In this case, the NH_4 demand for cell synthesis was approximated by the energy efficiency of hetero- and autotrophic bacteria that utilize NH_4 as the N source [*McCarty*, 1971; *Heijnen*, 2010]. This energy efficiency for NH_4 utilization for cell synthesis is typically set as 60% of available free energy generated from the respiratory pathways [*McCarty*, 1971; *Rittmann and McCarty*, 2001; *Xiao and Van Briesen*, 2005]. Thus, based upon this energy efficiency, we set y_{NH_4} equal to 0.4, such that $1 - y_{NH_4}$ of NH_4 in the system is used for cell synthesis demands (i.e., 40% of NH_4 is left available for nitrification). Inserting y_{O_2} and y_{NH_4} and the specified electron acceptors and donors for aerobic respiration, nitrification, and biological uptake reaction components into equation (4) yields

$$\begin{aligned} R_{O_2} = &-V_{O_2} y_{O_2} X_{AR} \left(\frac{DOC}{K_{DOC} + DOC}\right)\left(\frac{O_2}{K_{O_2} + O_2}\right) \\ &- V_{O_2}(1 - y_{O_2}) X_{NIT} \left(\frac{NH_4}{K_{NH_4} + NH_4}\right)\left(\frac{O_2}{K_{O_2} + O_2}\right), \end{aligned} \quad (9)$$

$$\begin{aligned} R_{NH_4} = &-V_{NH_4} y_{NH_4} X_{NIT} \left(\frac{NH_4}{K_{NH_4} + NH_4}\right)\left(\frac{O_2}{K_{O_2} + O_2}\right) \\ &- V_{NH_4}(1 - y_{NH_4}) X_{UP} \left(\frac{NH_4}{K_{NH_4} + NH_4}\right)\left(\frac{DOC}{K_{DOC} + DOC}\right), \end{aligned} \quad (10)$$

where, NH_4 is concentrations of ammonium (ML^{-3}), K_{NH_4} is the half-saturation constants for NH_4 (ML^{-3}), and the biomass X for each microbial functional groups are denoted by the subscripts NIT and UP for nitrification and biological uptake reaction components, respectively (ML^{-3}). The R_{NO_3} can now be represented as the sum of NO_3 produced via the nitrification component in equation (10) and the NO_3 removed via the denitrification component show in equation (7), such that

$$\begin{aligned} R_{NO_3} = &V_{NH_4} y_{NH_4} X_{NIT} \left(\frac{NH_4}{K_{NH_4} + NH_4}\right)\left(\frac{O_2}{K_{O_2} + O_2}\right) \\ &- V_{NH_3} X_{DN} I \left(\frac{DOC}{K_{DOC} + DOC}\right)\left(\frac{NO_3}{K_{NO_3} + NO_3}\right). \end{aligned} \quad (11)$$

[17] Using effective uptake rates for O_2 and NH_4 substantially reduced the Monod kinetic parameter space. Larger parameter space would decreases efficacy making more difficult the sensitivity analyses to identify key

kinetic parameters controlling net HZ nitrification and denitrification, which is a primary goal of this study. Reduced parameter space also allows us to represent the effective O_2 demand of aerobic respiration and nitrification and effective NH_4 demand of nitrification and microbial uptake as a function of O_2 and NH_4 availability. This approach is similar to the O_2 uptake rate used by *Marzadri et al.* [2011] that assumed total O_2 uptake rate equals the sum of aerobic respiration and nitrification rates. Unlike *Marzadri et al.* [2011], our approach does not assume that DOC or N substrates (i.e., K_{EA} and K_{ED} in equation (4)) are unlimited, which is important when considering large ranges in potential HZ DOC and N substrate conditions seen between semipristine and heavily polluted streams.

[18] Labile DOC is consumed during aerobic respiration, denitrification, and biological assimilation through cell synthesis (shown as CH_2O in Table 1). There are two possible sources of DOC in the model: (1) advected into the HZ with the O_2, NH_4, and NO_3, or (2) generated in situ via dissolution of particulate organic carbon (POC) located within the HZ sediment. Previous hyporheic studies have shown that POC can be advected into the HZ pore space [*Marmonier et al.*, 1995] or entrapped during flood events that mobilize the streambed [*Metzler and Smock*, 1990]. Furthermore, recent studies [*Gu et al.*, 2007; *Peyrard et al.*, 2011; *Zarnetske et al.*, 2011b] showed that in situ sources of DOC are necessary to explain observed denitrification rates in systems where DOC can be limiting (i.e., advection supplied DOC was inadequate to fuel the observed denitrification). Groundwater studies have shown that in situ POC sources, such as buried organic matter, release DOC as a kinetic process [*Robertson and Cherry*, 1995]. Therefore, the generation of DOC in situ was done with a POC kinetic dissolution model [e.g., *Jardine et al.*, 1992; *MacQuarrie* et al., 2001; *Gu et al.*, 2007]:

$$\frac{d\mathrm{POC}}{dt} = \alpha(k_d\mathrm{DOC} - \mathrm{POC}), \tag{12}$$

where POC is the homogeneously distributed POC mass in the sediment ($MM^{-1}_{\mathrm{sediment}}$), α is a first-order mass transfer coefficient (T^{-1}), and k_d is a linear distribution coefficient for the HZ sediment ($L^3M^{-1}_{\mathrm{sediment}}$). Therefore, the total DOC reaction R_{DOC} in the model is the sum of DOC produced in equation (12) and the DOC consumed by the aerobic respiration component, denitrification component, and biological assimilation through cell synthesis component, such that

$$\begin{aligned} R_{\mathrm{DOC}} = {} & \alpha(k_d\mathrm{DOC} - \mathrm{POC}) \\ & - V_{\mathrm{O_2}} y_{\mathrm{O_2}} X_{\mathrm{AR}} \left(\frac{\mathrm{DOC}}{K_{\mathrm{DOC}} + \mathrm{DOC}}\right)\left(\frac{\mathrm{O_2}}{K_{\mathrm{O_2}} + \mathrm{O_2}}\right) \\ & - V_{\mathrm{NH_4}}(1 - y_{\mathrm{NH_4}}) X_{\mathrm{UP}} \left(\frac{\mathrm{NH_4}}{K_{\mathrm{NH_4}} + \mathrm{NH_4}}\right)\left(\frac{\mathrm{DOC}}{K_{\mathrm{DOC}} + \mathrm{DOC}}\right) \\ & - V_{\mathrm{NO_3}} X_{\mathrm{DN}} I \left(\frac{\mathrm{DOC}}{K_{\mathrm{DOC}} + \mathrm{DOC}}\right)\left(\frac{\mathrm{NO_3}}{K_{\mathrm{NO_3}} + \mathrm{NO_3}}\right). \end{aligned} \tag{13}$$

2.1.1. Governing Equations

[19] The overall coupled nitrification and denitrification dynamics and one-dimensional (1-D) reactive solute transport modeled in this study are described by five coupled equations, one for each dissolved species (O_2, NH_4, NO_3, DOC) and one for the dissolution of POC. The governing equations of the model are

Dissolved Oxygen

$$\begin{aligned} \frac{\partial \mathrm{O_2}}{\partial t} = {} & D\frac{\partial^2 \mathrm{O_2}}{\partial x^2} - v\frac{\partial \mathrm{O_2}}{\partial x} - V_{\mathrm{O_2}} y_{\mathrm{O_2}} X_{\mathrm{AR}} \left(\frac{\mathrm{DOC}}{K_{\mathrm{DOC}} + \mathrm{DOC}}\right) \\ & \left(\frac{\mathrm{O_2}}{K_{\mathrm{O_2}} + \mathrm{O_2}}\right) - V_{\mathrm{O_2}}(1 - y_{\mathrm{O_2}}) X_{\mathrm{NIT}} \left(\frac{\mathrm{NH_4}}{K_{\mathrm{NH_4}} + \mathrm{NH_4}}\right)\left(\frac{\mathrm{O_2}}{K_{\mathrm{O_2}} + \mathrm{O_2}}\right). \end{aligned} \tag{14}$$

Ammonium

$$\begin{aligned} \frac{\partial \mathrm{NH_4}}{\partial t} = {} & D\frac{\partial^2 \mathrm{NH_4}}{\partial x^2} - v\frac{\partial \mathrm{NH_4}}{\partial x} - V_{\mathrm{NH_4}} y_{\mathrm{NH_4}} X_{\mathrm{NIT}} \left(\frac{\mathrm{NH_4}}{K_{\mathrm{NH_4}} + \mathrm{NH_4}}\right) \\ & \left(\frac{\mathrm{O_2}}{K_{\mathrm{O_2}} + \mathrm{O_2}}\right) - V_{\mathrm{NH_4}}(1 - y_{\mathrm{NH_4}}) X_{\mathrm{UP}} \left(\frac{\mathrm{NH_4}}{K_{\mathrm{NH_4}} + \mathrm{NH_4}}\right) \\ & \left(\frac{\mathrm{DOC}}{K_{\mathrm{DOC}} + \mathrm{DOC}}\right). \end{aligned} \tag{15}$$

Nitrate

$$\begin{aligned} \frac{\partial \mathrm{NH_3}}{\partial t} = {} & D\frac{\partial^2 \mathrm{NH_3}}{\partial x^2} - v\frac{\partial \mathrm{NH_3}}{\partial x} + V_{\mathrm{NH_4}} y_{\mathrm{NH_4}} X_{\mathrm{NIT}} \left(\frac{\mathrm{NH_4}}{K_{\mathrm{NH_4}} + \mathrm{NH_4}}\right) \\ & \left(\frac{\mathrm{O_2}}{K_{\mathrm{O_2}} + \mathrm{O_2}}\right) - V_{\mathrm{NH_3}} X_{\mathrm{DN}} I \left(\frac{\mathrm{DOC}}{K_{\mathrm{DOC}} + \mathrm{DOC}}\right)\left(\frac{\mathrm{NO_3}}{K_{\mathrm{NO_3}} + \mathrm{NO_3}}\right). \end{aligned} \tag{16}$$

Dissolved Organic Carbon

$$\begin{aligned} \frac{\partial \mathrm{DOC}}{\partial t} = {} & D\frac{\partial^2 \mathrm{DOC}}{\partial x^2} - v\frac{\partial \mathrm{DOC}}{\partial x} + \alpha(k_d\mathrm{DOC} - \mathrm{POC}) \\ & - V_{\mathrm{O_2}} y_{\mathrm{O_2}} X_{\mathrm{AR}} \left(\frac{\mathrm{DOC}}{K_{\mathrm{DOC}} + \mathrm{DOC}}\right)\left(\frac{\mathrm{O_2}}{K_{\mathrm{O_2}} + \mathrm{O_2}}\right) \\ & - V_{\mathrm{NH_4}}(1 - y_{\mathrm{NH_4}}) X_{\mathrm{UP}} \left(\frac{\mathrm{NH_4}}{K_{\mathrm{NH_4}} + \mathrm{NH_4}}\right)\left(\frac{\mathrm{DOC}}{K_{\mathrm{DOC}} + \mathrm{DOC}}\right) \\ & - V_{\mathrm{NO_3}} X_{\mathrm{DN}} I \left(\frac{\mathrm{DOC}}{K_{\mathrm{DOC}} + \mathrm{DOC}}\right)\left(\frac{\mathrm{NO_3}}{K_{\mathrm{NO_3}} + \mathrm{NO_3}}\right). \end{aligned} \tag{17}$$

Particulate Organic Carbon

$$\frac{d\mathrm{POC}}{dt} = \alpha(k_d\mathrm{DOC} - \mathrm{POC}). \tag{18}$$

All parameters have been defined previously, but also see the Notation section. Finally, we used a nondimensional form of the model equations to examine the role of rate-limiting processes across different hyporheic conditions and between systems [*Gu et al.*, 2007].

[20] The key assumptions used in deriving the transport and reaction terms in the model can be summarized as follows: (1) Dispersivity scales with the length of the system

as $\alpha_L = 0.02L$, which is representative of how α_L scales with L in groundwater systems [*Neumann*, 1990; *Gelhar et al.*, 1992]; α_L was fixed because it does not significantly influence the outcomes of steady state transport and because each additional parameter in Monte Carlo analyses increases the computational demands exponentially. (2) Multiple Monod kinetics is appropriate at the scale of a hyporheic zone. (3) Biomass growth and transport are negligible [*Bekins et. al.*, 1998]. (4) The dissolution of POC and the resorption of DOC are described by reversible first-order kinetics [*Jardine et al.*, 1992]. (5) All DOC is labile and bioavailable. (6) We use NH_4 to represent the end product of mineralized DON sources, and do not have a NH_4 source term. We do not include DON as a source term or state variable because there are many poorly defined intermediary reactions and pathways between DON and NH_4. However, it is well documented that NH_4 is readily converted to NO_3 in a single process—nitrification, so we represent the NH_4 as the direct source term for NO_3. We set the influent NH_4, O_2, NO_3, and DOC concentration to the concentrations observed in the stream during the *Zarnetske et al.* [2011a] study because those conditions exist in a known coupled nitrification-denitrification system. (7) Retardation due to sorption is negligible because we will solve the model at steady state. Retardation of these solutes can occur due to sorption processes in stream sediment and riparian systems [*Triska et al.*, 1994], and could be important in a transient model. (8) V_{O_2} and V_{NH_4} are specific rate coefficients that represent the cumulative effects of multiple microbial functional groups acting on a common solute. We assume that thermodynamic relationships can be used to represent the partitioning of O_2 and NH_4 uptake demand between aerobic respiration and nitrification and NH_4 demand via nitrification and biological uptake. The use of one effective reaction rate scaled by a partitioning coefficient for two metabolically mediated processes assumes that the different functional groups have the same reaction potential. This may not be appropriate for studies focused specifically on the nitrification pathway.

2.1.2. Numerical Solution and Model Conditions

[21] A second-order centered finite difference approximation was used to discretize the spatial derivatives in the steady state model for first- and second-order spatial derivatives. We let U represent a state variable in the model (e.g., $U = O_2$) and develop the general steady state form of the model. This general form is

$$\frac{\partial U}{\partial t} = 0 = \frac{\partial^2 U}{\partial x^2} - \frac{\partial U}{dx} - R(U), \tag{19}$$

$$U(0) = U_o \,(\text{inlet boundary condition}),$$

$$\left.\frac{\partial U}{\partial x}\right|_{x=1} = 0 \,(\text{outlet boundary condition}),$$

where $R(U)$ is the multiple Monod kinetic operator which is evaluated explicitly at the old values. A Dirichlet-type condition is used at the inlet of the model domain and a Neumann-type boundary condition at the outlet which is also estimated by a second-order approximation. For further details see *Zarnetske* [2011].

[22] Boundary and initial conditions were selected based upon the stream and hyporheic conditions observed by *Zarnetske et al.* [2011a]. The Dirichlet-type boundary condition of a specified concentration was used to represent the stream sourced solutes entering the model domain (i.e., head of lateral hyporheic flow paths). A Neumann-type boundary condition was used to represent advective transport of solutes out of the model domain (i.e., tail of lateral hyporheic flow paths). Using the Neumann-type boundary conditions assumes that the rate at which solute mass exits the flow path via dispersion is negligible and can be ignored in the model.

2.2. Hyporheic NO_3 Source-Sink Sensitivity Analysis

[23] We used a global Monte Carlo regional sensitivity analysis (RSA) to evaluate which model parameters were most important in controlling whether the hyporheic system generated a net increase (source) or decrease (sink) of NO_3 along a flow path. Thus, we defined the fractional change of NO_3 in the system, F_N (equation (2)) as a *pseudo* objective function for this RSA. We included 10 reaction parameters plus the mean advection water velocity v, so that residence time ($\tau = L/v$) can be evaluated (Table 2). Note that we did not include the biomass of the functional microbial groups facilitating the reactions (X) in the sensitivity analysis because they are implicitly included as lumped parameter in the model—it is a product with their respective microbial process reaction rates V_k [*Gu et al.*, 2007]. Consequently, the biomass values for X_{AR}, X_{NIT}, and X_{DN} were set as constants and equal to influent O_2, NH_4, and NO_3 for the global sensitivity analyses.

[24] The specific steps of the RSA used in this study are summarized below [for more detail see *Hornberger and Spear*, 1981; *Hornberger et al.*, 1985; *Wagener and Kollat*, 2007]. (1) Parameters from the model were selected for inclusion in the RSA (Table 2). (2) Literature values were used to identify the range of each parameter in the RSA (Table 2). (3) A uniform distribution bounded by the literature values was created for each parameter. (4) A series of Monte Carlo simulations were run ($n \geq 10{,}000$), where each simulation involves randomly sampling and recording a set of parameters from their uniform distributions. (5) For each simulation the F_N is calculated and recorded. (6) The sampled parameter sets for the simulations were then systematically partitioned into groups based upon their F_N behavior, i.e., parameter sets that produced either a source ($F_N > 1$) or sink ($F_N < 1$) of NO_3. We applied the *Freer et al.* [1996] RSA methodology within the Monte Carlo analysis toolbox (MCAT, *Wagener and Kollat* [2007]) to divide the parameter populations into 10 bins of equal size according to their F_N value. (7) The cumulative distributions of each binned parameter set were generated. The separation between these distributions of the source and sink curves indicate a difference in the properties of the N source and sink parameter values. For example, a large separation between distributions demonstrates that a parameter is sensitive because its value is strongly correlated with the model outcome. (8) The separation between the distribution curves of a parameter was quantified by using the Kolmogorov-Smirnov two-sample test [*Kottegoda and Rosso*, 1997]. The Kolmogorov-Smirnov two-sample test yields the maximum distance between the distributions ΔF_N, where the ΔF_N ranges between 0 and 1 and a ΔF_N close to 0 indicates an insensitive parameter. (9) The ΔF_N for each

Table 2. Model Parameters and Parameter Ranges Used in the Sensitivity Analyzes of This Study, Including Literature Sources[a]

Parameter	Units	Drift Creek Model	F_N Sensitivity Analysis Values	Source
Physical Parameters				
L	cm	500	500	24
v	cm h^{-1}	17.1	0.01–100	24
D	cm^2 h^{-1}	$0.02Lv$	$0.02Lv$	25, 26
Reaction Parameters				
V_{O_2}	h^{-1}	1.97	0.1–10.0	16, 21, 22, 23, 24
V_{NH_4}	h^{-1}	1.08	0.36–4.2	18, 20, 21, 22
V_{NO_3}	h^{-1}	3.98	0.26–10	3, 11, 15, 17, 18, 20, 21, 22
K_{O_2}	mg L^{-1}	5.28	0.2–5.8	5, 8, 14, 16, 17, 19, 20, 21, 22, 23
K_{DOC}	mg L^{-1}	8.68	1.0–10.0	5, 8, 14, 17, 21, 22
K_{NH_4}	mg L^{-1}	0.43	0.1–1.1	1, 2, 7, 9, 13, 21
K_{NO_3}	mg L^{-1}	1.64	0.21–3.1	3, 5, 8, 11, 14, 15, 17, 21, 22
K_I	mg L^{-1}	0.24	0.2–1.0	4, 5, 6, 8, 14, 17, 21, 22
α	h^{-1}	2.0×10^{-4}	1×10^{-5}–1×10^{-3}	10, 17, 22
k_d	L^3 kg^{-1}	50	5.0–100	12, 17, 22
y_{O_2}	–	0.64	0.64	27, 28, 29, 30
y_{NH_4}	–	0. 40	0. 40	30, 31, 32, 33

[a]Literature sources: 1. *Knowles et al.* [1965], 2. *McLaren* [1970], 3. *Messer and Brezonik* [1984], 4. *Tiedje* [1988], 5. *Kindred and Celia* [1989], 6. *Christensen and Tiedje* [1988], 7. *Gee et al.* [1990], 8. *Chen et al.* [1992], 9. *Drtil et al.* [1993], 10. *Jardine et al.* [1992], 11. *Schipper et al.* [1993], 12. *Robertson and Cherry* [1995], 13. *Stark* [1996], 14. *Doussan et al.* [1997], 15. *Maag et al.* [1997], 16. *Chen et al.* [1999], 17. *MacQuarrie et al.* [2001], 18. *Sheibley et al.* [2003], 19. *Robson and Hamilton* [2004], 20. *Romero et al.* [2004], 21. *Hedin et al.* [1998], 22. *Gu et al.* [2007], 23. *Higashino et al.* [2008], 24. *Zarnetske et al.* [2011a], 25. *Neuman* [1990], 26. *Gelhar et al.* [1992], 27. *Champ et al.*, 1979, 28. *Stumm and Morgan*, 1981, 29. *Hedin et al.*, 1998, 30. *Heijnen*, 2010, 31. *McCarty*, 1971, 32. *Rittmann and McCarty*, 2001, 33. *Xiao and Van Briesen*, 2005.

parameter is used to heuristically rank it relative to the other parameters in the sensitivity analysis with the most sensitive parameters having the largest ΔF_N and the least sensitive parameters having the smallest ΔF_N.

3. Results

3.1. Model Evaluation

[25] Prior to using the model to evaluate the hyporheic controls on the production (source) or removal (sink) of NO_3, the model was assessed with observation data from an instrumented parafluvial hyporheic zone in Drift Creek—an upland agricultural stream where both nitrification and denitrification are known to occur [*Zarnetske et al.*, 2011a]. The calibrated Drift Creek model was able to capture the dynamics of concentration profiles of all state-variables (O_2, NH_4, NO_3, and DOC) along the observed hyporheic flow paths (Figure 2; Table 2). The coupling of nitrification and denitrification in the model effectively simulated the nonlinear NO_3 concentration profiles. The observed DOC

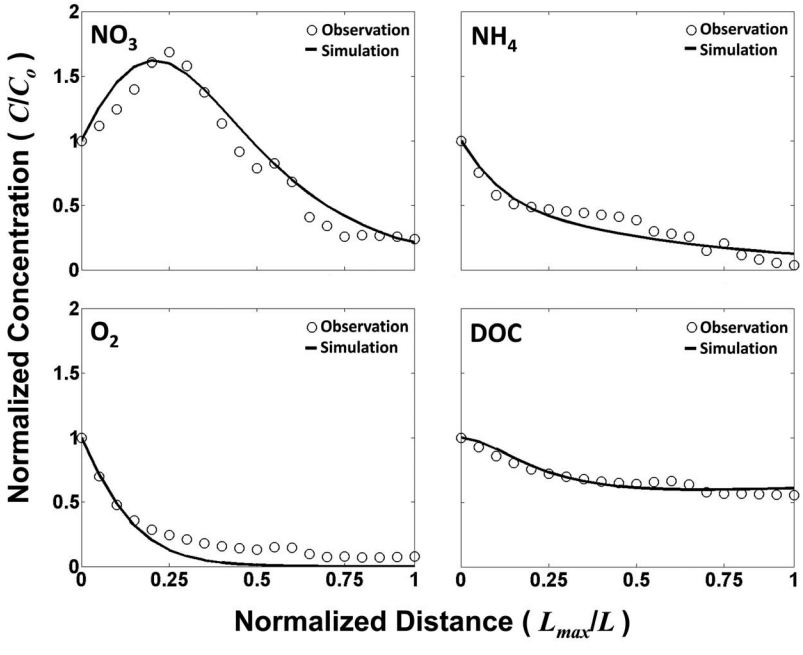

Figure 2. Observed (open circles) concentrations from a parafluvial hyporheic zone by *Zarnetske et al.* [2011a] versus the best-fit model simulations (solid lines). The $\overline{NSE}$ for the optimal simulations presented is 0.90.

persistence along the flow path was simulated with the POC dissolution model when coupled with the advected DOC sources. Details of the evaluation conditions and parameter estimation procedures are presented by *Zarnetske* [2011]. Overall, the best model fit was based upon simultaneously optimizing a Nash-Sutcliffe efficiency objective function *NSE* on all four state variables yielding a mean *NSE*, $\overline{NSE}$ of 0.90, where $\overline{NSE} = 1$ is a perfect model fit to the observed data [*Nash and Sutcliffe*, 1970].

3.2. Hyporheic NO_3 Source-Sink Analysis

[26] The model generated a suite of NO_3 source and sink simulations based on randomly selected hyporheic parameter sets. The subsequent global F_N based sensitivity analysis of these simulations showed that the effective uptake rate of O_2 and the advection rate were the two most influential parameters on the fate of inorganic N (i.e., the ΔF_N for $v = 0.68$, and $V_{O_2} = 0.55$; Table 3). The denitrification and nitrification reaction rates were also influential compared to the half-saturation constants and DOC supply parameters (i.e., the ΔF_N for $V_{NH_4} = 0.46$ and $V_{NO_3} = 0.43$).

[27] A set of Monte Carlo simulations conditioned on the influent stream solute concentrations observed in the HZ of a lateral gravel bar in Drift Creek, OR, USA (O_2 = 8.31 mg L^{-1}, NH_4 = 0.11 mg L^{-1}, NO_3 = 0.32 mg L^{-1}, and DOC = 3.01 mg L^{-1} [*Zarnetske et al.*, 2011a]) were conducted for the two most sensitive hyporheic parameters—physical advection rate v, and the biological O_2 uptake rate V_{O_2}. More specifically, these Monte Carlo simulations were sampled across the reported literature range for V_{O_2} while the range for v was selected to generate a range of residence times (τ = 0–1000 h). The other transport and reaction parameters were fixed at calibrated values [*Zarnetske*, 2011]. This resulting F_N response surface shows the range of possible combinations of NO_3 source-sink dynamics for the hyporheic parameters of V_{O_2} and τ (Figure 3) in Drift Creek. The F_N response illustrates that net nitrification can persist along flow paths when V_{O_2} is less than 1.05 h^{-1}. Conversely, net denitrification dominates most of the parameter space. The maximum net denitrification consistently occurs when the largest τ and V_{O_2} values are combined in the model.

[28] An additional set of more general stochastic Monte Carlo simulations with the nondimensional form of the model allowed us to evaluate a larger range of possible hyporheic conditions affecting NO_3 dynamics in streams. These simulations were again conditioned on influent solute conditions observed in *Zarnetske et al.* [2011a], but 11 physical and biogeochemical parameters were sampled across the reported literature ranges. These simulations yielded a wide range of net nitrification and net denitrification occurring along hyporheic flow paths. Some 82% of the 10,000 simulations resulted in net denitrification ($F_N < 1$) while only 18% resulted in net nitrification ($F_N > 1$). The resulting F_N for all 10,000 calculated Da_{O_2} values (Figure 4) shows dynamics similar to our hypothesis for hyporheic N dynamics (Figure 1), except that the initial NH_4 mass entering the hyporheic system limited the amount of potential nitrification at Da_{O_2} values less than 1, and the onset of denitrification was at Da_{O_2} values greater than 1. This shift in Da_{O_2} values for denitrification is associated with the additional residence time needed for denitrification to reduce the NO_3 generated via nitrification at earlier residence times. Still, the fraction of net nitrification ($F_N > 1$) outcomes to net denitrification ($F_N < 1$) outcomes occurring beyond calculated Da_{O_2} values shows a threshold with the fraction of $F_N > 1$ outcomes decreasing rapidly at $Da_{O_2} = 1$ and continuing to decrease with larger Da_{O_2} values (Figure 5).

Table 3. Hyporheic Nitrification-Denitrification Parameter Sensitivity Ranking Based Upon the Regional Sensitivity Analysis (RSA) With the Objective Function of F_N, the N Fractional Change (i.e., NO_3 Production or Removal)[a]

Parameter	Sensitivity Rank	ΔF_N
v	1	0.68
V_{O_2}	2	0.55
V_{NH_4}	4	0.46
V_{NO_3}	3	0.43
K_{NH_4}	9	0.37
K_{NO_3}	6	0.35
K_{DOC}	5	0.29
α	7	0.25
k_d	8	0.22
K_I	10	0.15
K_{O_2}	11	0.12

[a]The ΔF_N represents the parameter sensitivity as determined by the statistical Kolmogorov-Smirnov test of the RSA results.

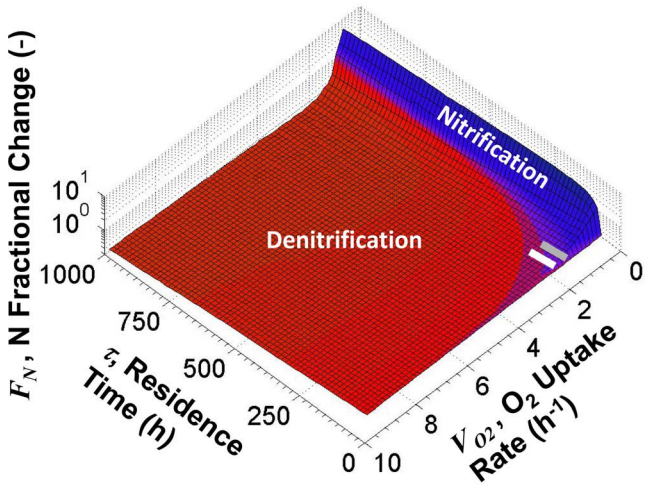

Figure 3. The F_N response surface of the Drift Creek hyporheic zone for varying oxygen uptake rate V_{O_2}, and residence time τ, showing the net nitrification domain ($F_N > 1$) in blue and net denitrification domain ($F_N < 1$) in red. The white box on the F_N response surface shows the observed parameter domain measured during a 2007 field investigations of the hyporheic zone by *Zarnetske et al.* [2011a], which observed coupled nitrification and denitrification across hyporheic residence times. Similarly, the gray box shows conditions during a 2008 field investigation when O_2 uptake and denitrification were more limited by labile DOC supply [*Zarnetske et al.*, 2011b].

4. Discussion

4.1. Transport and Reaction Kinetics Control N Source-Sink Dynamics

[29] The numerical simulations show that Damköhler number for dissolved O_2, the ratio of the characteristic

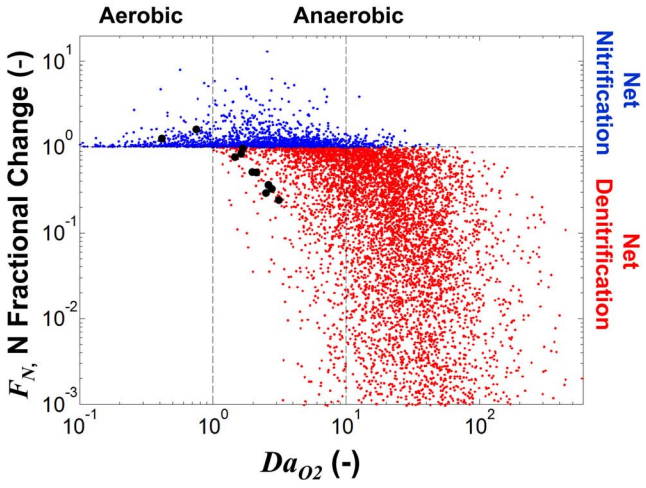

Figure 4. The relationship between F_N and Da_{O_2} based upon 10,000 stochastically generated simulations using biogeochemical reaction parameter values bounded by known literature ranges. Net nitrification simulations are shown as blue dots and net denitrification simulations are shown as red dots. Large black dots show data from 11 hyporheic well locations of Drift Creek [*Zarnetske et al.*, 2011a]. Note the general agreement of the simulations with the hypothesized solution space shown in Figure 1 and represented by the solid curves.

residence time scale and O_2 uptake time scale, presents a useful framework from which to estimate the net nitrification or denitrification potential of hyporheic zones. The effectiveness of combining the transport conditions with the O_2 uptake conditions to predict NO_3 source and sink processes in this study is not surprising. From a physical transport perspective, our findings show that the transport rate and residence time (i.e., the solute supply time scales) are the most important factors in determining the fate of NO_3. This finding is in agreement with previous observation and modeling studies of reactive NO_3 transport in HZs

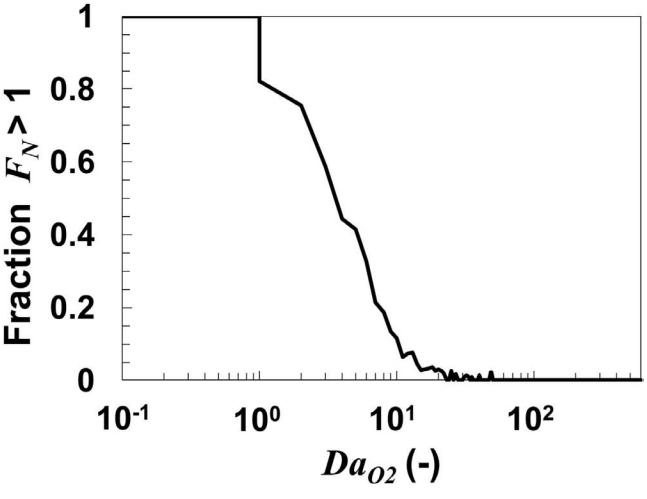

Figure 5. The fraction of simulations with $F_N > 1$ (i.e., net nitrification) occurring across Da_{O2} values. All values based upon the 10,000 stochastic hyporheic NO_3 model simulations shown in Figure 4.

[e.g., *Gu et al.*, 2007; *Cardenas et al.*, 2008; *Boano et al.*, 2010; *Marzadri et al.*, 2011, *Zarnetske et al.*, 2011a; *Bardini et al.*, 2012]. This strong and consistent relationship between the fate of NO_3 and residence time suggests that the approach of using a Lagrangian framework [*Boano et al.*, 2010; *Marzadri et al.*, 2011] should be pursued in future models of groundwater–surface water NO_3 dynamics. From a biogeochemical and thermodynamic perspective this study shows that Da_{O_2} can serve as a proxy for defining NO_3 source and sink systems, because the microbial redox reaction energy released during the respiration of NO_3 is second only to O_2 in microbial respiration processes (free energy: aerobic respiration = 501 kJ and denitrification = 476 kJ [*Hedin et al.*, 1998]). Therefore, the use of O_2 dynamics as a first-order approximation of the onset of denitrification is theoretically justified and may make spatiotemporal comparisons of N source-sink dynamics more feasible (see section 4.2). However, while the use of Da_{O_2} to predict other redox reactions maybe possible, it becomes less certain because the thermodynamic advantage of microbes to utilize other terminal electron acceptors, such as Mn(IV), Fe(III), SO_4, is much less than O_2.

4.1.1. Nitrification and Denitrification Dynamics and Limitations

[30] Net nitrification will be reaction rate limited along hyporheic flow paths with $Da_{O_2} < 1$ because O_2 is present. The reaction rate may be limited by other factors such as the number of reaction sites available, the amount of NH_4 available, the temperature, or pH. At $Da_{O_2} > 1$ nitrification will become limited by the availability of O_2, because the supply rate of O_2 is less than biological demand. Figure 1 shows that net nitrification can occur over the entire Da_{O_2} domain if the right combination of reaction substrate is available. For example, a flow path with maximum nitrification would contain: (1) a large source O_2, (2) a large source of DON to mineralize into NH_4, (3) a small concentration of NO_3 such that denitrifier communities may not be readily recruited to the system, and (4) a small concentration of labile DOC such that aerobic respiration of O_2 would be limited, leaving more O_2 for nitrification.

[31] Net denitrification will be transport limited along hyporheic flow paths with $Da_{O_2} < 1$ because denitrification will be inhibited by the physical supply of O_2. For $Da_{O_2} < 1$ the bulk of the water will be oxic and have the potential to fuel nitrification. In this $Da_{O_2} < 1$ domain, denitrification would be restricted to microsites where anaerobic conditions can develop [*Holmes et al.*, 1996; *Zarnetske et al.*, 2011a], however, the net effect of denitrification in this Da_{O_2} domain will be limited. Conversely, at points in a system where $Da_{O_2} > 1$, denitrification will dominate until it becomes substrate limited, because O_2 inhibition will no longer exist. At $Da_{O_2} > 1$, substrate and chemical factors such as NO_3 and labile DOC availability, temperature, and pH will become the dominant controls on denitrification rates.

4.1.2. Coupled Nitrification and Denitrification Dynamics

[32] Nitrification and denitrification were strongly coupled along the flow path in the stochastic modeling results (Figure 4). As seen in previous hyporheic studies [e.g., *Sheibley et al.*, 2003; *Zarnetske et al.*, 2011a; *Marzadri et al.*, 2011], tracking O_2 and NO_3 concentrations along flow paths show that a parcel of water can experience coupled

nitrification and denitrification (i.e., previous observations show distributions of F_N going from low Da_{O_2} to high Da_{O_2}; see dotted line in Figure 1 and gray and white boxes in Figure 3 based on *Zarnetske et al.* [2011a] field data). Initially the parcel of water travels along the head of the flow paths (low Da_{O_2} values) and will experience nitrification which consumes O_2 and increases NO_3 mass. Therefore, the nitrification and aerobic respiration acting on that parcel of water promotes denitrification–anaerobic conditions and increased NO_3 concentrations. So as the parcel of water spends more time in the system traveling toward the distal end of the flow paths (high Da_{O_2} values), denitrification will start to dominate and NO_3 mass will decrease. In the stochastic hyporheic simulations, the onset of net denitrification did not consistently occur at the originally hypothesized $Da_{O_2} = 1$, but at values closer to $Da_{O_2} = 10$ (Figures 4 and 5). This can be explained by the process of coupled nitrification and denitrification, because net denitrification ($F_N < 1$) cannot occur until the additional NO_3 mass generated during nitrification is denitrified. This additional denitrification will require longer residence times in the reactive system resulting in larger Da_{O_2} values. If a stream had low hyporheic nitrification rates due to little to no available DON or NH_4, such as the streams in Antarctica [*Gooseff et al.*, 2004; *Koch et al.*, 2010], then we might expect to see net denitrification occurring closer to $Da_{O_2} = 1$. Conversely, large amounts of nitrification may be possible at $Da_{O_2} < 1$ in streams where there are high concentrations of NH_4 in the surface waters (i.e., unlike the Drift Creek example and results in Figure 4). These high nitrification potentials will shift net denitrification to much larger time scales. Furthermore, modeling studies that do not account for the potential effects of nitrification when modeling hyporheic NO_3 dynamics [e.g., *Gu et al.*, 2007; *Boano et al.*, 2010] will have limited applicability because they cannot represent the NO_3 source potential of HZs and may misrepresent the true time scales and rates of denitrification.

[33] The numerical modeling and sensitivity analyses also indicate that future nitrification-denitrification modeling efforts may not require all of the reaction kinetic parameters involved in the present study. For example, across the stochastic hyporheic simulations, the half-saturation constants of the Monod kinetics and the O_2 inhibition term were less influential than the reaction rate constants in determining the nitrification and denitrification dynamics (Table 3). This suggests that if the goal is to predict net nitrification or denitrification conditions of a hyporheic zone, simpler expressions of the reaction kinetics (e.g., zero- and first-order kinetic models) may be capable of capturing the basic behavior of nitrification and denitrification while reducing the parsimony of the model. For example, inspection of equation (4) shows that, if we can assume electron donors and acceptors are not limiting in our study system (e.g., $C_{ED} \gg K_{ED}$), the Monod kinetic model reduces to the zero-order model $R_i \approx V_k$. Alternatively, if we know if electron donors or acceptors are limited in the study system (e.g., $C_{ED} \ll K_{ED}$), the Monod kinetic term becomes the first-order model $R_i \approx k_i C_{ED}$, where k_i is a rate coefficient. These simplifying kinetic assumptions were employed by *Sheibley et al.* [2003] to successfully simulate the inorganic N transformations in hyporheic profusion cores of an N-limited system, albeit without comparison to alternative forms of the Monod kinetic model. Similarly, the recent mechanistic modeling studies by *Marzadri et al.* [2011] and *Bardini et al.* [2012] also assumed simplified reaction kinetics (i.e., first-order) for inorganic N species, O_2, and DOC. Our detailed analysis with multiple Monod kinetics provides additional support for the reaction kinetic assumptions used in their models.

[34] There are additional factors not directly accounted for in the numerical modeling and the Da_{O_2} approach, such as actual labile DOC supply, temperature, and pH. These additional factors will ultimately dictate how tightly coupled in space and time the nitrification and denitrification domains are [*Jones and Holmes*, 1996; *Duff and Triska*, 2000]. Still the Da_{O_2} approach seems to indirectly capture most of this complexity and offers a simplified framework for assessing the role of hyporheic zones on stream N cycling.

4.2. Assessing Hyporheic NO_3 Source-Sink Function

[35] Stream hydraulic conditions, including surface flow, bed hydraulic conductivity, and channel geometry, control the characteristic hyporheic time scales and residence time distributions [e.g., *Haggerty et al.*, 2002; *Kasahara and Wondzell*, 2003; *Boano et al.*, 2006; *Cardenas*, 2008]. Therefore these channel features are important controls on the Da_{O_2} dynamics of a stream HZ. To illustrate this point, we applied the Da_{O_2} concept to a well-documented parafluvial HZ where coupled nitrification and denitrification was observed along flow paths (Figure 6 inset; Drift Creek, OR, USA [see *Zarnetske et al.*, 2011a]). We used a groundwater flow model parameterized with surface flow, bed hydraulic

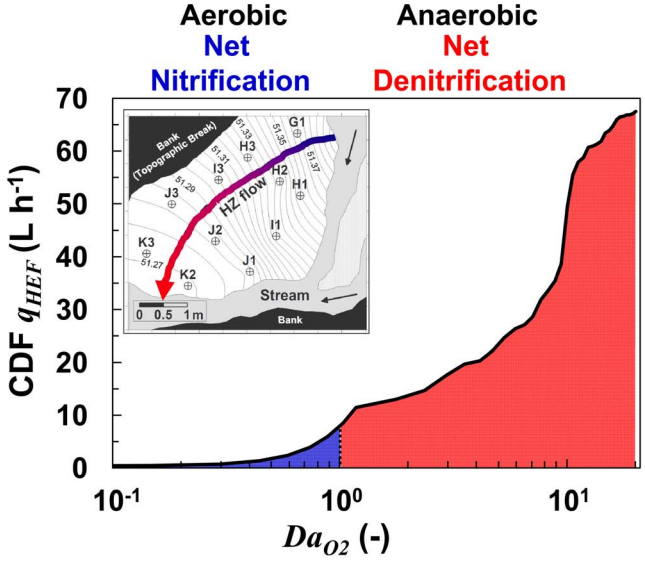

Figure 6. The cumulative distribution of specific hyporheic exchange flow (q_{HEF}) as a function of the modeled Da_{O_2} distribution for the Drift Creek hyporheic study site based on 2007 data when there was known coupled nitrification and denitrification conditions. Overall, the majority of the q_{HEF} has a potential function of a net sink for NO_3 in the stream due to denitrification (see red shaded region beyond set Da_{O_2} threshold of 1). The inset map shows the groundwater model domain and the lateral hyporheic exchange at the Drift Creek gravel bar site.

conductivity, porosity, and channel-hyporheic geometry to estimate the residence time distribution as well as the specific hyporheic exchange flow q_{HEF} associated with different residence times [see *Zarnetske*, 2011 for details]. The modeled residence times were coupled with field measures of V_{O_2} to produce a distribution of Da_{O_2} as well as quantify the different portions of the q_{HEF} that have a potential for net nitrification or denitrification (Figure 6). Based upon this application of Da_{O_2}, we are able to quantify the distribution of q_{HEF} as a net source and a sink of NO_3 to the surface waters of Drift Creek at the time of the initial study. Based upon this Da_{O_2} analysis it is estimated that 91% of the q_{HEF} at the Drift Creek study site is functioning as a net sink of NO_3.

[36] The ability to quantify the ecosystem function of HZs in terms of regulating the flux of reactive N is becoming more feasible. Improvements are being made in predicting HZ residence times based upon simple stream network conditions, such as channel slope and hydraulic conductivity [e.g., *Cardenas at al.* 2008; *Wondzell*, 2011; *Tonina and Buffington*, 2011]. Therefore, these modeling approaches may lead to effective ways of quantifying residence time dynamics across sites without extensive data acquisition and model computation demands. It will also facilitate the coupling of biogeochemical reaction time scales with transport time scales to model hyporheic solute dynamics, such as in the Da_{O_2} approach. Furthermore, these new models of residence times may enable stream channel restoration projects to design for characteristic residence time scales [*Hester and Gooseff*, 2010; *O'Connor et al.*, 2010; *Ward et al.*, 2011], which can be coupled with the Da_{O_2} approach to estimate the potential hyporheic net source or sink NO_3 function of the restored streams.

[37] The Da_{O_2} concept is also promising because field measurements of in situ dissolved O_2 uptake dynamics are now readily obtainable and more affordable than measurements of reactive forms of dissolved N because O_2 concentrations can be measured with field deployable and data logging probes systems (e.g., optical O_2 measurement technologies). Furthermore, there are analytical and empirical model approaches to quantify O_2 uptake rates [e.g., *Rutherford et al.*, 1995; *Higashino et al.*, 2008; *O'Connor et al.*, 2009; *González-Pinzón et al.*, 2012]. These models of HZ O_2 dynamics may offer an elegant way to couple O_2 dynamics with the physical hydrologic models of HZ residence times. Thereby, directly coupling biogeochemical kinetic models with the hydrologic kinetic models—an approach that offers an opportunity to make predictions about complex ecosystem processes such as the NO_3 source or sink function of existing or designed hyporheic environments.

5. Conclusions

[38] We demonstrate in this study that the characteristic hyporheic transport and reaction rate time scales will determine when and where net nitrification and denitrification will occur in a system and when each process is either transport or reaction rate limited. The stochastic models of widely varying hyporheic transport and reaction rate conditions showed that the key controls on the fate of reactive inorganic N and hyporheic redox conditions is primarily governed by the residence time of the solute in the system and the O_2 uptake rate. Furthermore, these two parameters can be measured or modeled in future investigations and related to each other in a useful way via the dimensionless Damköhler number for O_2, Da_{O_2}, which is simply the ratio of the characteristic residence time scale and O_2 uptake time scale. This Da_{O_2} is fundamentally a way to determine the net aerobic-anaerobic conditions of groundwater–surface water exchange environments. Furthermore, as demonstrated for a parafluvial hyporheic zone, the Da_{O_2} approach can be extended to incorporate the effects of an entire residences time distribution on the net aerobic-anaerobic conditions and N source-sink function of groundwater–surface water exchange. This study also indicates that simplified kinetic models and empirical methods that link residence time and O_2 uptake time scales are useful for predicting the fate of N in future groundwater–surface water studies. Overall, Da_{O_2} is a useful scaling approach for evaluating different streams hyporheic zones and groundwater–surface water exchange flow paths to each other—across space and time, and may help make predictions about the hyporheic functioning as either a source or a sink of reactive inorganic N in a given stream.

Notation

α	first-order mass transfer coefficient (T^{-1}).
α_L	dispersivity (L).
C	concentration of solute (ML^{-3}).
D	dispersion coefficient (L^2T^{-1}).
Da_{O_2}	Damköhler number for dissolved oxygen (–).
DOC	concentration of dissolved organic carbon (ML^{-3}).
EA	electron acceptor.
ED	electron donor.
F_N	fraction change in nitrate mass (–)
ΔF_N	maximum distance between parameter distributions (–).
ΔG^o_{AR}	free energy yield of aerobic respiration reaction ($ML^2T^{-2}\text{mol}^{-1}$).
ΔG^o_{NIT}	free energy yield of nitrification reaction ($ML^2T^{-2}\text{mol}^{-1}$).
I	noncompetitive uptake inhibition of denitrification reaction (–).
k_d	linear distribution coefficient of sediment ($L^3M^{-1}_{\text{sediment}}$).
K	half-saturation constant (ML^{-3}).
K_{DOC}	half-saturation constants for dissolved organic carbon (ML^{-3}).
K_{NH_4}	half-saturation constant for ammonium (ML^{-3}).
K_{NO_3}	half-saturation constant for nitrate (ML^{-3}).
K_{O_2}	half-saturation constants for dissolved oxygen (ML^{-3}).
K_I	inhibition constant for the denitrification reaction (ML^{-3}).
L	length of the flow path (L).
N_{in}	concentration of nitrate at the beginning of flow path (ML^{-3}).
N_{out}	concentration of nitrate at the end of flow path (ML^{-3}).
NH_4	concentration of ammonium (ML^{-3}).
NO_3	concentration of nitrate (ML^{-3}).
O_2	concentrations of dissolved oxygen (ML^{-3}).

POC	particulate organic carbon in sediment ($MM^{-1}_{\text{sediment}}$).
q_{HEF}	specific hyporheic exchange flow (L^3T^{-1}).
R	total biological reaction rate term ($ML^{-3}T^{-1}$).
$R^*_{O_2}$	aerobic respiration component reaction rate ($ML^{-3}T^{-1}$).
$R^*_{NO_3}$	denitrification component reaction rate ($ML^{-3}T^{-1}$).
R_{O_2}	total biological dissolved oxygen reaction rate ($ML^{-3}T^{-1}$).
R_{NH_4}	total biological ammonium reaction rate ($ML^{-3}T^{-1}$).
R_{NO_3}	total biological nitrate reaction rate ($ML^{-3}T^{-1}$).
R_{DOC}	total biological dissolved organic carbon reaction rate ($ML^{-3}T^{-1}$).
τ	water residence time (T).
U	state variable in numerical model (e.g., O_2).
v	mean advected water velocity (LT^{-1}).
V	maximum specific microbial process reaction rate (T^{-1}).
V_{NH_4}	maximum specific ammonium reaction rate (T^{-1}).
V_{NH_3}	maximum specific denitrification rate (T^{-1}).
V_{O_2}	maximum specific oxygen reaction rate (T^{-1}).
X	biomass of a functional microbial group (ML^{-3}).
X_{AR}	biomass of the aerobic respiration functional group (ML^{-3}).
X_{DN}	biomass of the denitrifiers (ML^{-3}).
X_{NIT}	biomass of the nitrifiers (ML^{-3}).
X_{UP}	biomass of the ammonium assimilating microbes (ML^{-3}).
y_{NH_4}	partition coefficient for ammonium demand process components (–).
y_{O_2}	partition coefficient for dissolved oxygen demand process components (–).

[39] **Acknowledgments.** Support for this project was provided by a NSF Ecosystem Informatics IGERT fellowship (NSF grant DGE-0333257) to J.P.Z., research grants from the OSU Institute for Water and Watersheds and a Society for Freshwater Sciences Endowment Fund to J.P.Z., and the NSF grant EAR-0409534 to R.H. and S.M.W. V.A.B. would like to acknowledge the NSF Mathematical Biology grant DMS-1122699 for partial support. Further research support was provided by the Hollis M. Dole Environmental Geology Foundation at OSU and NSF Grant EAR-0838338. Discussions with C. Gu and S. Gregory greatly enhanced this study. We also thank the AE and four anonymous reviewers who provided insightful comments that improved this manuscript. Any opinions, findings and conclusions, or recommendations expressed in this material are those of the authors and do not necessarily reflect the views of the NSF.

References

Arango, C. P., and J. L. Tank (2008), Land use influences the spatiotemporal controls on nitrification and denitrification in headwater streams, *J. North Am. Benthol. Soc.*, *27*, 90–107.

Baker, M. A., C. N. Dahm, and H. M. Valett (2000a), Nitrogen biogeochemistry and surface-subsurface exchange in streams, in *Streams and Ground Waters*, edited by J. A. Jones and P. J. Mulholland, pp. 259–283, Academic, San Diego.

Baker, M. A., H. M. Valett, and C. N. Dahm (2000b), Organic carbon supply and metabolism in a shallow groundwater ecosystem, *Ecology*, *81*, 3133–3148.

Bardini, L., F. Boano, M. B. Cardenas, R. Revelli, and L. Ridolfi (2012), Nutrient cycling in bedform induced hyporheic zones, *Geochim. Cosmochim. Acta*, *84*, 47–61.

Bekins, B. A., E. Warren, and E. M. Godsy (1998), A comparison of zero-order, first-order, and Monod biotransformation models, *Ground Water*, *36*, 261–268.

Boano, F., C. Camporeale, R. Revelli, and L. Ridolfi (2006), Sinuosity-driven hyporheic exchange in meandering rivers, *Geophys. Res. Lett.*, *33*(18), L18406, doi:10.1029/2006GL027630.

Boano, F., A. Demaria, R. Revelli, and L. Ridolfi (2010), Biogeochemical zonation due to intrameander hyporheic flow, *Water Resour. Res.*, *46*, W02511, doi:10.1029/2008WR007583.

Boucher, D. F., and G. E. Alves (1959), *Dimensionless Numbers for Fluid Mechanics, Heat Transfer, Mass Transfer, and Chemical Reaction*, pp. 55–64, Chemical Engineering Progress, New York.

Burgin, A. J., and S. K. Hamilton (2007), Have we overemphasized the role of denitrification in aquatic ecosystems? A review of nitrate removal pathways, *Frontiers Ecol. Environ.*, *5*(2), 89–96.

Cardenas, M. B. (2008), Surface water-groundwater interface geomorphology leads to scaling of residence times, *Geophys. Res. Lett.*, *35*(8), L08402, doi:10.1029/2008GL033753.

Cardenas, M. B., et al. (2008), Constraining denitrification in permeable wave-influenced marine sediment using linked hydrodynamic and biogeochemical modeling, *Earth Planet. Sci. Lett.*, *275*, 127–137.

Champ, D. R., J. Gulens, and R. E. Jackson (1979), Oxidation-reduction sequences in ground-water flow systems, *Can. J. Earth Sci.*, *16*, 12–23.

Chen, G. H., I. M. Leong, J. Liu, and J. C. Huang (1999), Study of oxygen uptake by tidal river sediment, *Water Res.*, *33*, 2905–2912.

Chen, Y. M., L. M. Abriola, P. J. J. Alvarez, P. J. Anid, and T. M. Vogel (1992), Modeling transport and biodegradation of benzene and toluene in sandy aquifer material—Comparisons with experimental measurements, *Water Resour. Res.*, *28*(7), 1833–1847, doi:10.1029/92WR00667.

Christensen, P. B., L. P. Nielsen, J. Sorensen, and N. P. Revsbech (1990), Denitrification in nitrate-rich streams—Diurnal and seasonal-variation related to benthic oxygen-metabolism, *Limnol. Oceanogr.*, *35*, 640–651.

Christensen, S., and J. M. Tiedje (1988), Oxygen control prevents denitrifiers and barley plant-roots from directly competing for nitrate, *FEMS Microbiol. Ecol.*, *53*, 217–221.

Diaz, R. J., and R. Rosenberg (2008), Spreading dead zones and consequences for marine ecosystems, *Science*, *321*, 926–929.

Domenico, P. A., and F. W. Schwartz (1998), *Physical and Chemical Hydrogeology*, 2nd ed., 506 pp., John Wiley, New York.

Doussan, C., G. Poitevin, E. Ledoux, and M. Detay (1997), River bank filtration: Modelling of the changes in water chemistry with emphasis on nitrogen species, *J. Contam. Hydrol.*, *25*, 129–156.

Drtil, M., P. Nemeth, and I. Bodik (1993), Kinetic constants of nitrification, *Water Res.*, *27*, 35–39.

Duff, J. H., and F. J. Triska (1990), Denitrification in sediments from the hyporheic zone adjacent to a small forested stream, *Can. J. Fish. Aquat. Sci.*, *47*, 1140–1147.

Duff, J. H., and F. J. Triska (2000), Nitrogen biogeochemistry and surface-subsurface exchange in streams, in *Streams and Ground Waters*, edited by J. A. Jones and P. J. Mulholland, pp. 197–217, Academic, San Diego.

Freer, J., K. Beven, and B. Ambroise (1996), Bayesian estimation of uncertainty in runoff prediction and the value of data: An application of the GLUE approach, *Water Resour. Res.*, *32*, 2161–2173, doi:10.1029/95WR03715.

Gee, C. S., M. T. Suidan, and J. T. Pfeffer (1990), Modeling of nitrification under substrate-inhibiting conditions, *J. Environ. Eng.*, *116*, 18–31.

Gelhar, L. W., C. Welty, and K. R. Rehfeldt (1992), A critical-review of data on field-scale dispersion in aquifers, *Water Resour. Res.*, *28*, 1955–1974, doi:10.1029/92WR00607.

González-Pinzón, R., R. Haggerty, and D. Myrold (2012), Measuring aerobic respiration in stream ecosystems using the resazurin-resorufin system, *J. Geophys. Res.*, *117*, G00N06, doi:10.1029/2012JG001965.

Gooseff, M. N., D. M. McKnight, R. L. Runkel, and J. H. Duff (2004), Denitrification and hydrologic transient storage in a glacial meltwater stream, McMurdo Dry Valleys, Antarctica, *Limnol. Oceanogr.*, *49*, 1884–1895.

Gruber, N., and J. N. Galloway (2008), An Earth-system perspective of the global nitrogen cycle, *Nature*, *451*, 293–296.

Gu, C. H., G. M. Hornberger, A. L. Mills, J. S. Herman, and S. A. Flewelling (2007), Nitrate reduction in streambed sediments: Effects of flow and biogeochemical kinetics, *Water Resour. Res.*, *43*(12), W12413, doi:10.1029/2007WR006027.

Haggerty, R., S. M. Wondzell, and M. A. Johnson (2002), Power-law residence time distribution in the hyporheic zone of a 2nd-order mountain stream, *Geophys. Res. Lett.*, *29*(13), 1640, doi:10.1029/2002GL014743.

Hedin, L. O., J. C. von Fischer, N. E. Ostrom, B. P. Kennedy, M. G. Brown, and G. P. Robertson (1998), Thermodynamic constraints on nitrogen transformations and other biogeochemical processes at soil-stream interfaces, *Ecology*, *79*, 684–703.

Heijnen, J. J. (2010), Impact of thermodynamic principles in systems biology, *Adv. Biochem. Eng./Biotechnol.*, *121*, 139–162.

Heijnen, J. J., and Van Dijken J. P. (1992), In search of a thermodynamic description of biomass yields for the chemotrophic growth of microorganisms, *Biotechnol. Bioeng.*, *39*(8), 833–858.

Hester, E. T., and M. N. Gooseff (2010), Moving beyond the banks: Hyporheic restoration is fundamental to restoring ecological services and functions of streams, *Environ. Sci. Technol.*, *44*, 1521–1525.

Higashino, M., B. O'Connor, M. Hondzo, and H. Stefan (2008), Oxygen transfer from flowing water to microbes in an organic sediment bed, *Hydrobiologia*, *614*, 219–231.

Holmes, R. M., S. G. Fisher, and N. B. Grimm (1994), Parafluvial nitrogen dynamics in a desert stream ecosystem, *J. North Am. Benthol. Soc.*, *13*, 468–478.

Holmes, R. M., J. B. Jones, S. G. Fisher, and N. B. Grimm (1996), Denitrification in a nitrogen-limited stream ecosystem, *Biogeochemistry*, *33*, 125–146.

Hornberger, G. M., and R. C. Spear (1981), An approach to the preliminary-analysis of environmental systems, *J. Environ. Manage.*, *12*, 7–18.

Hornberger, G. M., K. J. Beven, B. J. Cosby, and D. E. Sappington (1985), Shenandoah watershed study—Calibration of a topography-based, variable contributing area hydrological model to a small forested catchment, *Water Resour. Res.*, *21*, 1841–1850.

Inwood, S. E., J. L. Tank, and M. J. Bernot (2005), Patterns of denitrification associated with land use in 9 midwestern headwater streams, *J. North Am. Benthol. Soc.*, *24*, 227–245.

Jardine, P. M., F. M. Dunnivant, H. M. Selim, and J. F. McCarthy (1992), Comparison of models for describing the transport of dissolved organic carbon in aquifer columns, *Soil Sci. Soc. Am. J.*, *56*, 393–401.

Jones, J. B., and R. M. Holmes (1996), Surface-subsurface interactions in stream ecosystems, *Trends Ecol. Evol.*, *11*, 239–242.

Kasahara, T., and S. M. Wondzell (2003), Geomorphic controls on hyporheic exchange flow in mountain streams, *Water Resour. Res.*, *39*(1), 1005, doi:10.1029/2002WR001386.

Kelso, B. H. L., R. V. Smith, and R. J. Laughlin (1999), Effects of carbon substrate on nitrite accumulation in freshwater sediments, *Appl. Environ. Microbiol.*, *65*, 61–66.

Kindred, J. S., and M. A. Celia (1989), Contaminant transport and biodegradation: 2. Conceptual-model and test simulations, *Water Resour. Res.*, *25*, 1149–1159, doi:10.1029/WR025i006p01149.

Knowles, G., A. L. Downing, and M. J. Barrett (1965), Determination of kinetic constants for nitrifying bacteria in mixed culture with aid of an electronic computer, *J. Gen. Microbiol.*, *38*, 263–278.

Koch, J. C., D. M. McKnight, and J. L. Baeseman (2010), Effect of unsteady flow on nitrate loss in an oligotrophic, glacial meltwater stream, *J. Geophys. Res.*, *115*, G01001, doi:10.1029/2009JG001030.

Kottegoda, N. T., and R. Rosso (1997), *Applied Statistics for Civil and Environmental Engineers*, McGraw-Hill, New York.

Maag, M., M. Malinovsky, and S. M. Nielsen (1997), Kinetics and temperature dependence of potential denitrification in riparian soils, *J. Environ. Qual.*, *26*, 215–223.

MacQuarrie, K. T. B., E. A. Sudicky, and W. D. Robertson (2001), Numerical simulation of a fine-grained denitrification layer for removing septic system nitrate from shallow groundwater, *J. Contam. Hydrol.*, *52*, 29–55.

Marmonier, P., D. Fontvieille, J. Gibert, and V. Vanek (1995), Distribution of dissolved organic carbon and bacteria at the interface between the Rhone River and its alluvial aquifer, *J. North Am. Benthol. Soc.*, *14*, 382–392.

Marzadri, A., D. Tonina, and A. Bellin (2011), A semi-analytical three-dimensional process-based model for hyporheic nitrogen dynamics in gravel bed rivers, *Water Resour. Res.*, *47*, W11518, doi:10.1029/2011WR010583.

McCarty, P. L. (1971), Energentics and bacterial growth, in *Organic Compounds in Aquatic Environments.* edited by S. D. Faust and J. V. Hunter, pp. 495–532, Marcel Dekker, New York.

McLaren, A. D. (1970), Temporal and vectorial reactions of nitrogen in soil—A review, *Can. J. Soil Sci.*, *50*, 97–109.

Messer, J. J., and P. L. Brezonik (1984), Laboratory evaluation of kinetic-parameters for lake sediment denitrification models, *Ecolog. Model.*, *21*, 277–286.

Metzler, G. M., and L. A. Smock (1990), Storage and dynamics of subsurface detritus in a sand-bottomed stream, *Can. J. Fish. Aquat. Sci.*, *47*, 588–594.

Molz, F. J., M. A. Widdowson, and L. D. Benefield (1986), Simulation of microbial-growth dynamics coupled to nutrient and oxygen-transport in porous media, *Water Resour. Res.*, *22*(8), 1207–1216, doi:10.1029/WR022i008p01207.

Nash, J. E., and J. V. Sutcliffe (1970), River flow forecasting through conceptual models part I: A discussion of principles, *J. Hydrol.*, *10*(3), 282–290.

Neuman, S. P. (1990), Universal scaling of hydraulic conductivities and dispersivities in geologic media, *Water Resour. Res.*, *26*(8), 1749–1758, doi:10.1029/WR026i008p01749.

Ocampo, C. J., C. E. Oldham, and M. Sivapalan (2006), Nitrate attenuation in agricultural catchments: Shifting balances between transport and reaction, *Water Resour. Res.*, *42*, W01408, doi:10.1029/2004WR003773.

O'Connor, B. L., M. Hondzo, and J. W. Harvey (2009), Incorporating physical and kinetic limitations in quantifying dissolved oxygen flux to aquatic sediments, *J. Environ. Eng.*, *135*(12), 1304–1314, doi:10.1061/_ASCE_EE.1943-7870.0000093.

O'Connor, B., M. Hondzo, and J. W. Harvey (2010), Predictive modeling of transient storage and nutrient uptake: Implications for stream restoration, *J. Hydraul. Eng.*, *136*(12), 1018–1032.

Peyrard, D., S. Delmotte, S. Sauvage, P. Namour, M. Gerino, P. Vervier, and J. M. Sanchez-Perez (2011), Longitudinal transformation of nitrogen and carbon in the hyporheic zone of an N-rich stream: A combined modeling and field study, *Phys. Chem. Earth*, *36*(12), 599–611, doi:10.1016/j.pce.2011.05.003.

Pinay, G., T. C. O'Keefe, R. T. Edwards, and R. J. Naiman (2009), Nitrate removal in the hyporheic zone of a salmon river in Alaska, *River Res. Appl.*, *25*, 367–375.

Puckett, L. J., C. Zamora, H. Essaid, J. T. Wilson, H. M. Johnson, M. J. Brayton, and J. R. Vogel (2008), Transport and fate of nitrate at the ground-water/surface-water interface, *J. Environ. Qual.*, *37*, 1034–1050.

Pusch, M., and J. Schwoerbel (1994), Community respiration in hyporheic sediments of a mountain stream (Steina, Black-Forest), *Archiv Hydrobiol.*, *130*, 35–52.

Rittmann, B. E., and P. L. McCarty (2001), *Environmental Biotechnology: Principles and Applications*, McGraw-Hill, New York.

Robertson, W. D., and J. A. Cherry (1995), In-situ denitrification of septic-system nitrate using reactive porous-media barriers—Field trials, *Ground Water*, *33*, 99–111.

Robson, B. J., and D. P. Hamilton (2004), Three-dimensional modelling of a Microcystis bloom event in the Swan River estuary, Western Australia, *Ecol. Model.*, *174*, 203–222.

Romero, J. R., J. P. Antenucci, and J. Imberger (2004), One- and three-dimensional biogeochemical simulations of two differing reservoirs, *Ecol. Model.*, *174*, 143–160.

Rutherford, J. C., J. D. Boyle, A. H. Elliott, T. V. J. Hatherell, and T. W. Chiu (1995), Modeling benthic oxygen uptake by pumping, *J. Environ. Eng.*, *121*, 84–95.

Sala, O. E., et al. (2000), Global biodiversity scenarios for the Year 2100, *Science*, *287*, 1770–1774.

Schipper, L. A., A. B. Cooper, C. G. Harfoot, and W. J. Dyck (1993), Regulators of denitrification in an organic riparian soil, *Soil Biol. Biochem.*, *25*, 925–933.

Segel, I. H. (1975), *Enzyme Kinetics*, 957 pp., John Wiley, New York.

Seitzinger, S. P. (1988), Denitrification in fresh-water and coastal marine ecosystems—Ecological and geochemical significance, *Limnol. Oceanogr.*, *33*, 702–724.

Seitzinger, S., J. A. Harrison, J. K. Bohlke, A. F. Bouwman, R. Lowrance, B. Peterson, C. Tobias, and G. Van Drecht (2006), Denitrification across landscapes and waterscapes: A synthesis, *Ecol. Appl.*, *16*, 2064–2090.

Sheibley, R. W., A. P. Jackman, J. H. Duff, and F. J. Triska (2003), Numerical modeling of coupled nitrification-denitrification in sediment perfusion cores from the hyporheic zone of the Shingobee River, MN, *Adv. Water Resour.*, *26*, 977–987.

Smith, V. H. (2003), Eutrophication of freshwater and coastal marine ecosystems—A global problem, *Environ. Sci. Pollut. Res.*, *10*, 126–139.

Sobczak, W. V., S. Findlay, and S. Dye (2003), Relationships between DOC bioavailability and nitrate removal in an upland stream: An experimental approach, *Biogeochemistry*, *62*, 309–327.

Stark, J. M. (1996), Modeling the temperature response of nitrification, *Biogeochemistry*, *35*, 433–445.

Stumm, W., and J. J. Morgan (1981), *Aquatic Chemistry: An Introduction Emphasizing Chemical Equilibria in Natural Waters*, John Wiley, New York.

Terry, R. E., and D. W. Nelson (1975), Factors influencing nitrate transformations in sediments, *J. Environ. Qual.*, *4*, 549–554.

Tiedje, J. M. (1988), Ecology of denitrification and dissimilatory nitrate reduction to ammonium, in *Environmental Microbiology of Anaerobes*, edited by A. J. B. Zehnder, pp. 179–244, John Wiley, New York.

Tonina, D., and J. M. Buffington (2011), Effects of stream discharge, alluvial depth and bar amplitude on hyporheic flow in pool-riffle channels, *Water Resour. Res.*, *47*, W08508, doi:10.1029/2010WR009140.

Triska, F. J., A. P. Jackman, J. H. Duff, and R. J. Avanzino (1994), Ammonium sorption to channel and riparian sediments—A transient storage pool for dissolved inorganic nitrogen, *Biogeochemistry*, *26*(2), 67–83.

van Kessel, J. F. (1977), Factors affecting the denitrification rate in two water-sediment systems, *Water Res.*, *11*(3), 259–267.

Wagener, T., and J. Kollat (2007), Numerical and visual evaluation of hydrological and environmental models using the Monte Carlo analysis toolbox, *Environ. Model. Software*, *22*, 1021–1033.

Ward, A. S., M. N. Gooseff, and P. A. Johnson (2011), How can subsurface modifications to hydraulic conductivity be designed as stream restoration structures? Analysis of Vaux's conceptual models to enhance hyporheic exchange, *Water Resour. Res.*, *47*, W08512, doi:10.1029/2010WR010028.

Wondzell, S. M. (2011), The role of the hyporheic zone across stream networks, *Hydrol. Processes*, *25*, 3525–3532.

Xiao, J., and J. M. Van Briesen (2005), Expanded thermodynamic model for microbial true yield prediction, *Biotechnol. Bioeng.*, *93*(1), 110–121, doi:10.1002/bit.20700.

Zarnetske, J. P. (2011), Hydrological and biogeochemical dynamics of nitrate production and removal at the stream–groundwater interface, Ph.D. thesis, 173 pp., Oregon State University, Corvallis, (http://ir.library.oregonstate.edu/xmlui/handle/1957/23463).

Zarnetske, J. P., R. Haggerty, S. M. Wondzell, and M. A. Baker (2011a), Dynamics of nitrate production and removal as a function of residence time in the hyporheic zone, *J. Geophys. Res.*, *116*, G01025, doi:10.1029/2010JG001356.

Zarnetske, J. P., R. Haggerty, S. M. Wondzell, and M. A. Baker (2011b), Labile dissolved organic carbon supply limits hyporheic denitrification, *J. Geophys. Res.*, *116*, G04036, doi:10.1029/2011JG001730.